A Digital Holographic Approach for Co-Phasing of Segmented Telescopes: Proof of Concept Using Numerical Simulations

Author(s): Changwei Li and Sijiong Zhang

Source: *Publications of the Astronomical Society of the Pacific*, Vol. 126, No. 937 (March 2014), pp. 280-286
Published by: The University of Chicago Press on behalf of the Astronomical Society of the Pacific
Stable URL: http://www.jstor.org/stable/10.1086/675973
Accessed: 03/04/2014 23:37

PUBLICATIONS OF THE ASTRONOMICAL SOCIETY OF THE PACIFIC, **126**:280–286, 2014 March

A Digital Holographic Approach for Co-Phasing of Segmented Telescopes: Proof of Concept Using Numerical Simulations

CHANGWEI LI[1,2] AND SIJIONG ZHANG[1,2]

Received 2013 December 04; accepted 2014 February 14; published 2014 March 5

ABSTRACT. Online co-phasing of segmented telescopes by dual-wavelength digital holography is proposed. Two digital holograms (one hologram per wavelength) are employed to get the phase of the segmented telescope for a longer synthetic wavelength by the digital holographic approach. The holograms are recorded by a high-speed CCD camera using the point-diffraction Mach-Zehnder interferometer. By fitting the plane for the synthetic wavelength phase in each segment of the telescope, the coefficients of piston and tip/tilt for each segment can be acquired. To test the feasibility of the proposed method, two simulated telescopes with 37 hexagonal segments are taken as examples to examine co-phasing segmented telescopes by digital holography when atmospheric turbulence and detection noises exist. Numerical simulations show that the dual-wavelength digital holographic approach for co-phasing of segmented telescopes is feasible and highly accurate and robust.

Online material: color figure

1. INTRODUCTION

For segmented telescopes, the main problem is co-phasing the individual segments of the telescopes to provide diffraction-limited image quality for the detection of dim objects in deep space. To solve this problem, several optical techniques have been proposed and developed. Interferometric techniques, the most traditionally used optical method, are employed to measure the phase of segmented telescopes by analyzing either the fringe mismatch (Pizarro et al. 2002) or the fringe difference between two complementary interferograms (Yaitskova et al. 2005). Wavefront sensing methods, techniques widely used in adaptive optics, are applied to sense wavefronts of segmented telescopes using different wavefront reconstructions (Orlov et al. 2000; Esposito et al. 2003) and retrieval algorithms (Li and Zhang, 2012). Phase-diverse phase retrieval, an optimization method, is used to find the phase of the telescope that best matches two degraded images by an iterative gradient search algorithm (Paxman & Fienup 1988). The diffraction methods, successfully used in the Keck telescope, are managed to measure the phase of segmented telescopes by analyzing the images produced by a lenslet array situated in the conjugate plane of the telescope pupil (Chanan et al. 1998, 2000). Within the narrowband technique of the diffraction methods, the problem of absolute phase ambiguity has been resolved by making measurements at two different wavelengths to obtain the phase at a longer synthetic wavelength (Chanan et al. 1998).

In the past decades, the digital holography technique has been proposed for phase measurements and compensation in high-resolution microscopy (Yamaguchi et al. 2001; Mann et al. 2005; Charrière et al. 2006). The outstanding advantage of the digital holographic technique in phase measurement is extending the range of phase measurements by numerical processing of holograms to acquire the phases of objects at longer synthetic wavelengths (Gass et al. 2003; Mann et al. 2008).

Here, the dual-wavelength digital holographic technique is proposed for online co-phasing of segmented telescopes. By using this technique, the range of the phase measurements for co-phasing segmented telescopes can be extended. The paper is structured as follows: Section 2 shows the principle of dual-wavelength digital holography for co-phasing of segmented telescopes. The experimental configuration using the point-diffraction Mach-Zehnder interferometer for co-phasing of segmented telescopes by digital holography is presented in § 3. In § 4, the numerical experimental results of co-phasing for two simulated segmented telescopes are shown and discussed. Finally, the conclusions for co-phasing the simulated telescopes by dual-wavelength digital holography are given.

2. PRINCIPLE

The principle of co-phasing segmented telescopes by dual-wavelength digital holography is based on two off-axis holograms (a small offset angle between the reference and object beams), one hologram per wavelength, which is acquired by

[1] National Astronomical Observatories/Nanjing Institute of Astronomical Optics and Technology, Chinese Academy of Sciences, Nanjing 210042, China; sjzhang@niaot.ac.cn.

[2] Key Laboratory of Astronomical Optics and Technology, Nanjing Institute of Astronomical Optics and Technology, Chinese Academy of Sciences, Nanjing 210042, China.

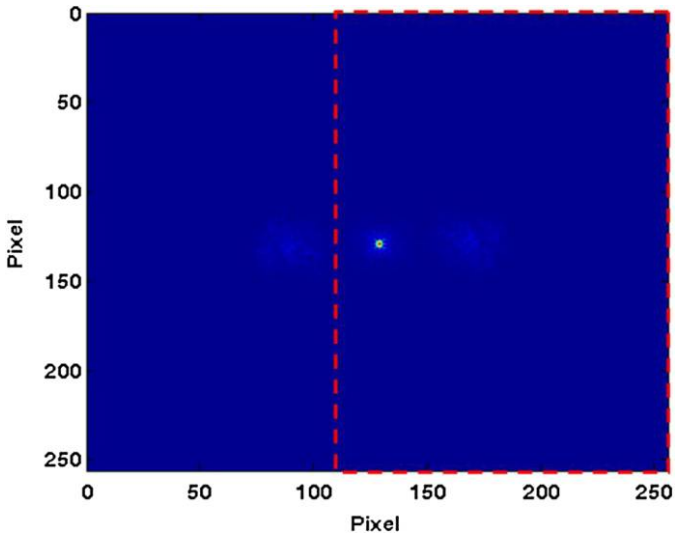

FIG. 1.—Schematic diagram of the operation of the digital filter. The spectrum values at frequencies in the red dashed rectangle are set to zero. See the electronic edition of the *PASP* for a color version of this figure.

a high-speed CCD camera using the point-diffraction Mach-Zehnder interferometer. The interferograms recorded at the two different wavelengths can be written as:

$$I_{H1}(x,y) = |O_1|^2 + |R_1|^2 + O_1R_1^* + O_1^*R_1,$$
$$I_{H2}(x,y) = |O_2|^2 + |R_2|^2 + O_2R_2^* + O_2^*R_2, \quad (1)$$

where O stands for the object beam containing the phase information of the segmented telescopes, R is the reference, the superscript $*$ is the complex conjugate, and the subscripts 1 and 2 stand for the two different wavelengths λ_1 and λ_2, respectively.

To obtain the phase of segmented telescopes, the procedures are follows: First, the Fourier spectrum, $\mathcal{F}(I_{H1})/\mathcal{F}(I_{H2})$ (see eq. [2] below), for each interferogram of the corresponding wavelength is obtained from the Fourier transform. As a linear phase shift caused by the small offset angle in the space domain introduces a translation in the Fourier frequency domain, the spectrum containing the phase information of the telescope can be moved away from the low frequency Fourier spectral components in the Fourier plane. Then, the spectrum containing the phase information of the original segmented telescope in each Fourier spectrum of the corresponding wavelength can be filtered out by a digital filter, SF (see eq. [2] below). Third, for each wavelength, the light-field distribution, E_1/E_2 (see eq. [2] below), containing the phase of the telescope is acquired by multiplying the inverse Fourier transform of the filtered spectra obtained by the second step with the complex conjugate of the light field, Tip_1^*/Tip_2^* (see eq. [2] below), caused by the offset angle. Finally, the phase of the segmented telescope for a synthetic wavelength can be extracted by multiplying the light-field distribution E_1 for one wavelength with the complex conjugate of the light-field distribution E_2 for the other wavelength. According to this procedure, the light-field distributions at two different wavelengths can be mathematically expressed as:

$$E_1 = \mathcal{F}^{-1}\{SF[\mathcal{F}(I_{H1})]\}Tip_1^*,$$
$$E_2 = \mathcal{F}^{-1}\{SF[\mathcal{F}(I_{H2})]\}Tip_2^*, \quad (2)$$

where $\mathcal{F}^{-1}$ is the inverse Fourier transform, $\mathcal{F}$ is the Fourier transform, SF stands for a digital filter, *Tip* is the light field caused by the offset angle. Figure 1 offers a schematic diagram of the operation of the digital filter SF. The cutoff of the SF filter is set at the minimum intensity between the telescope

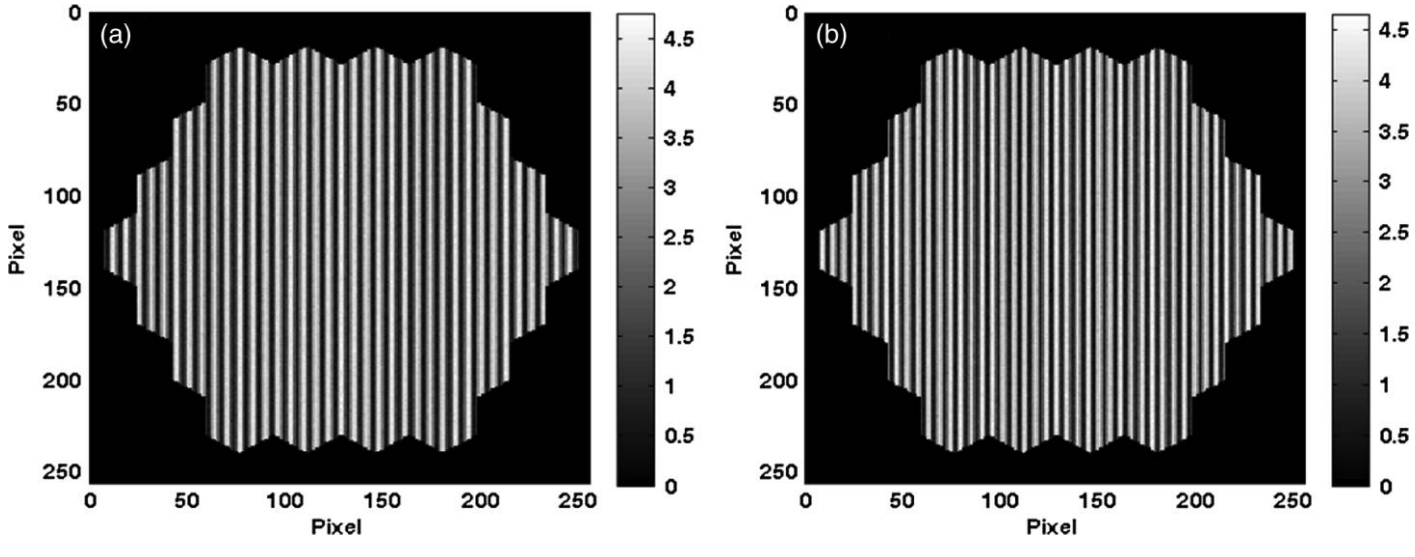

FIG. 2.—Holograms of (*a*) Tip_1 and (*b*) Tip_2.

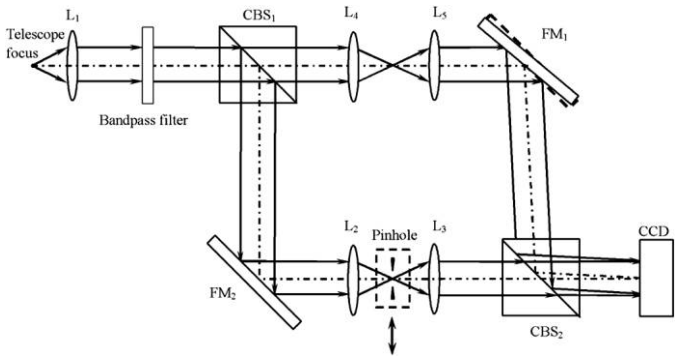

FIG. 3.—Experimental configuration for co-phasing of segmented telescopes by digital holography: CBS_1, CBS_2 = cubic beam splitters; L_1–L_5 = lenses; FM_1, FM_2 = flatmirrors.

spectrum and the halo in the center. Hence, only the phase information of the telescope is retained, and any redundant information is eliminated. As shown in Figure 1, the spectrum in the red dashed rectangle is set to zero. By multiplying the complex conjugate of *Tip*, a frequency shift in the Fourier plane can be avoided during extraction of the phase of the segmented telescope.

For the sake of acquiring the light field *Tip*, the interferogram of *Tip* for each wavelength is recorded by removing the pinhole from the optical layout. To avoid confusion, the two interferograms of *Tip* at the wavelengths of λ_1 and λ_2 are expressed as I^t_{H1} and I^t_{H2}, respectively. As the interferograms I^t_{H1} and I^t_{H2}, shown in Figure 2, only contain the phase information of *Tip*, the light-field distribution of Tip_1 and Tip_2 can be obtained by:

$$Tip_1 = \mathcal{F}^{-1}\{SF[\mathcal{F}(I^t_{H1})]\}, \qquad Tip_2 = \mathcal{F}^{-1}\{SF[\mathcal{F}(I^t_{H2})]\}. \tag{3}$$

How to get the two interferograms of *Tip* will be described in § 3.

With the light-field distributions calculated by equation (2), the phase of the segmented telescope at a longer synthetic wavelength can be obtained:

$$\Delta\varphi = \arg[E_1(E_2)^*] = \frac{2\pi}{\lambda'} z(x, y), \tag{4}$$

where $\lambda' = \lambda_1\lambda_2/|\lambda_1 - \lambda_2|$ is the synthetic wavelength, and $z(x, y)$ is the height error along the optics axis at point (x, y). Obviously, the smaller the difference between λ_1 and λ_2, the longer the synthetic wavelength will be. Hence, if the synthetic wavelength is long enough, the phase of the segmented telescopes at the synthetic wavelength can be determined without ambiguity according to equation (4).

To overcome errors caused by atmospheric turbulence and measurement noises, the piston and tip/tilt coefficients for each segment are acquired by fitting the plane into the retrieved synthetic wavelength phase for each segment of the telescope. For phase plane fitting in each segment, a central region that does not contain either edge of this segment is selected. The influence of the Gibbs phenomenon at the intersegments can be avoided. In this region selected for each segment of the telescope, the piston coefficient is extracted by averaging many frame phases over the selected region, and tip/tilt coefficients are obtained by fitting and averaging the phase plane using:

$$\Delta\varphi^s_i(x, y) = A_i x + B_i y + C_i, \tag{5}$$

where $\Delta\varphi^s_i(x, y)$ is the phase in the selected region for the segment i at point (x, y), A_i and B_i are the tip/tilt coefficients, and C_i is the piston coefficient. Note that the coefficients A_i, B_i and C_i must be converted to coefficients of height errors $z^s_i(x, y)$ by

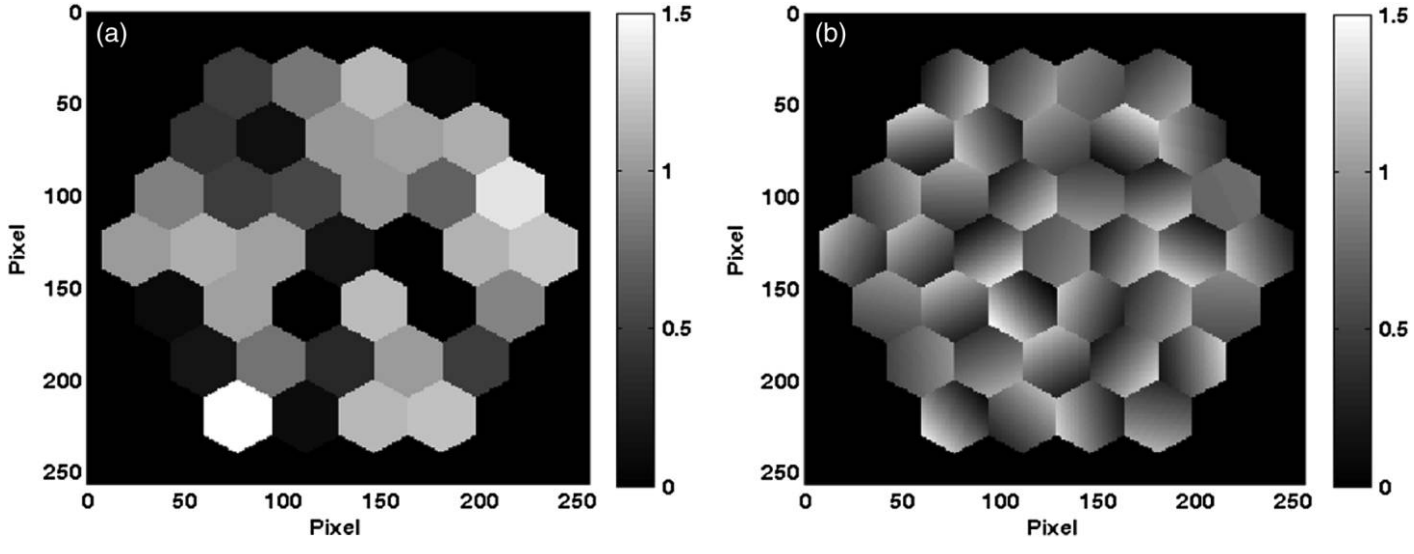

FIG. 4.—Two simulated telescopes of (*a*) T1 and (*b*) T2; scales are in microns.

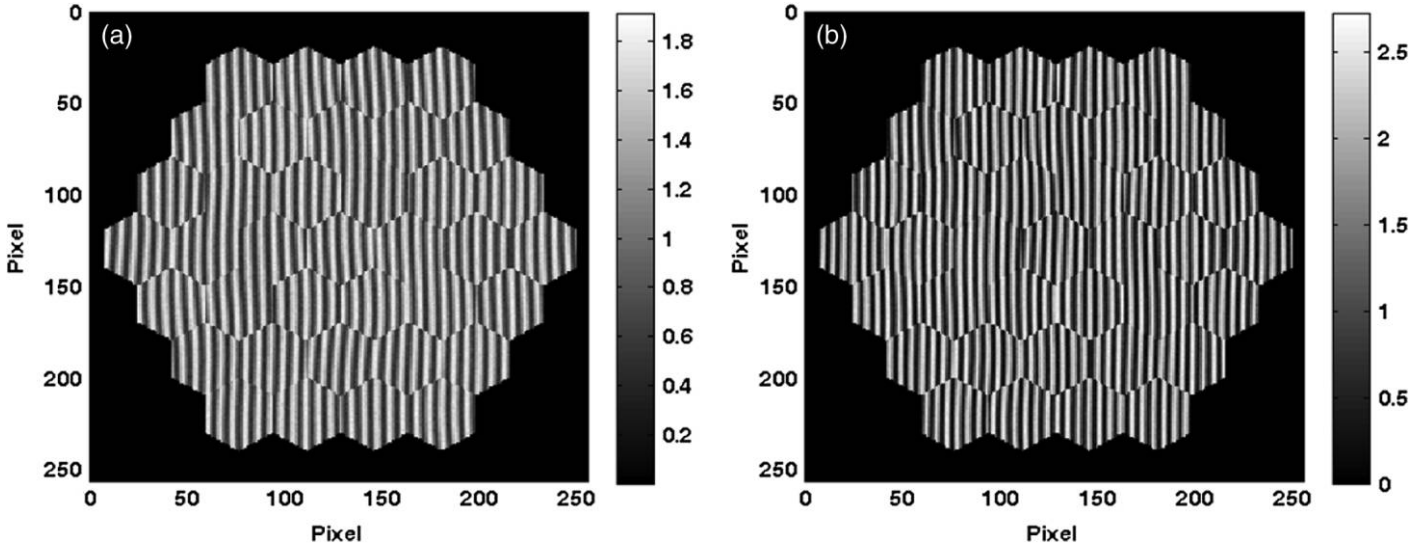

FIG. 5.—Holograms for T1 recorded at the wavelengths of (*a*) 0.632 μm and (*b*) 0.532 μm, with S/N = 20.

multiplication with the factor $\lambda'/(2\pi)$. Moreover, in order to co-phase segmented telescopes with high accuracy, the above procedure for co-phasing segmented telescopes needs to be repeated about 3 times or more.

3. EXPERIMENTAL CONFIGURATION

The experimental configuration, shown in Figure 3, is the point-diffraction Mach-Zehnder interferometer for co-phasing of segmented telescopes by digital holography. A divergent beam from the focus of a segmented telescope is collimated by a convex lens. Narrow bandpass filters are located behind the collimated lens to obtain beams with the wavelengths of interest. The point-diffraction Mach-Zehnder interferometer generates off-axis interferograms by introducing a small offset angle between two arms using a flat mirror, FM_1 (see Fig. 3, *dashed line*). In one arm of the interferometer, a pinhole located at the focal plane of L_2 and L_3 acting as a spatial filter provides the reference beam interfering with the beam in the other arm (Angel 1994). To balance the interferometer, two lenses identical to those in the reference arm are inserted in the other arm (the object arm). Moreover, by inserting two lenses in the object arm, rotational interference can be avoided when removing the pinhole from the optical layout to acquire interferograms of *Tip*. The beams in the two arms are recombined by a cubic beam splitter to generate interferograms recorded by a high-speed CCD camera. The minimum exposure time of the CCD camera must be smaller than the coherence time of the turbulence.

Using the above experimental configuration for co-phasing of segmented telescopes, steps are performed as follows:

1. First, remove the pinhole from the optical layout using a translation stage and, for each wavelength, record the interferogram, which only contains the phase information of *Tip*.

2. Then, put the pinhole back in the original position and acquire the interferograms containing the phase information of the segmented telescope.

3. Finally, co-phasing of the segmented telescope can be performed according to the procedures described in § 2.

4. NUMERICAL EXPERIMENTAL RESULTS AND DISCUSSION

In order to test the feasibility of online co-phasing segmented telescopes by dual-wavelength digital holography, two simulated telescopes with 37 hexagonal segments are used. One only contains piston errors (abbreviated T1 hereafter), and the other

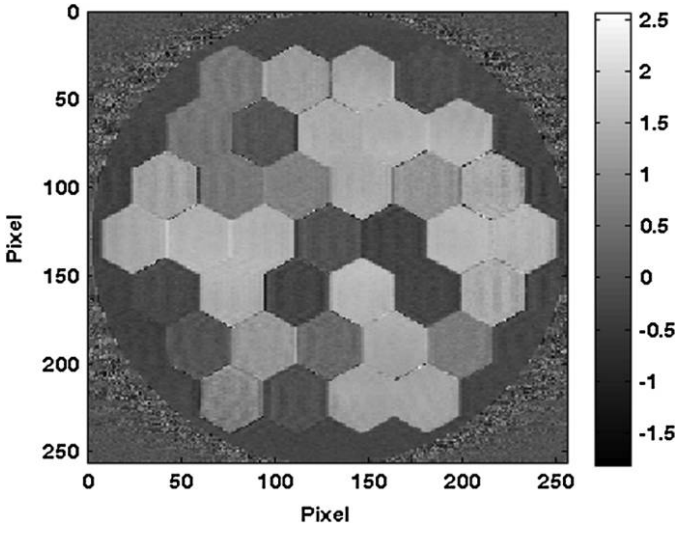

FIG. 6.—Averaged height error of T1 at the synthetic wavelength; the scale is in radians.

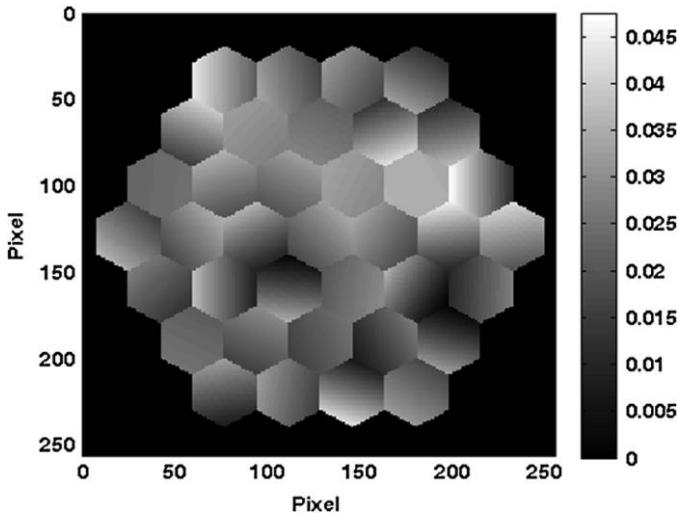

FIG. 7.—Residual height error of T1; the scale is in microns.

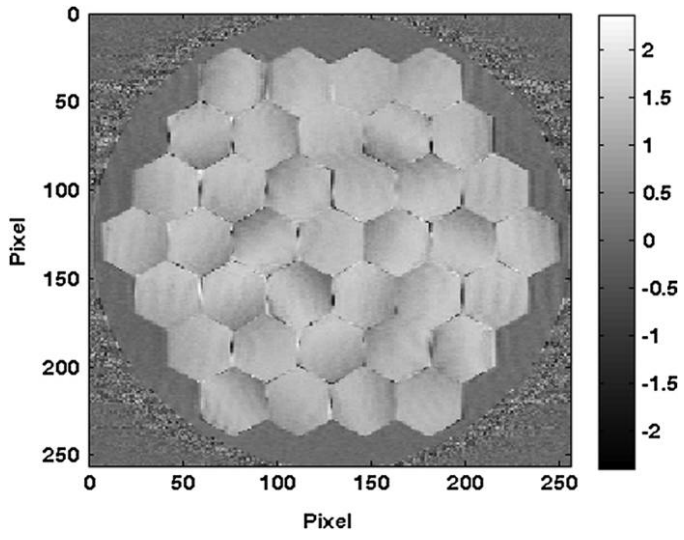

FIG. 9.—Averaged height error of T2 at the synthetic wavelength; the scale is in radians.

one contains both piston and tip/tilt errors (abbreviated T2 hereafter). T1, with a peak-to-valley (PV) value of 1.50 μm and a root mean square (rms) value of 0.450 μm is shown in Figure 4*a*, and T2, with a PV value of 1.50 μm and an rms value of 0.226 μm, is shown in Figure 4*b*.

The interferograms of T1 and T2 are acquired at the wavelengths of 0.633 and 0.532 μm in the presence of atmospheric turbulence and detection noises. For each wavelength, 500 turbulence phase screens with averaged PV values of 0.6 waves are applied to successively disturb the fringe pattern of the interferometer, and 500 interferograms, each containing the phase information of both the telescope and a phase screen, are recorded by a high-speed CCD. For each interferogram, a random white Gaussian noise is added according to the definition of the signal-to-noise ratio (S/N; Roggemann et al. 1992).

4.1. Co-Phasing of T1 by Dual-Wavelength Digital Holography

Two interferograms, which contain the phase information of T1 at the wavelengths of 0.633 and 0.532 μm with S/N = 20, are shown in Figure 5. As only piston errors are included in T1, the fringe orientations in each segment for T1 are almost the same as those of *Tip*. Moreover, the fringe spacing of the interferogram at the wavelength of 0.633 μm is wider than that at

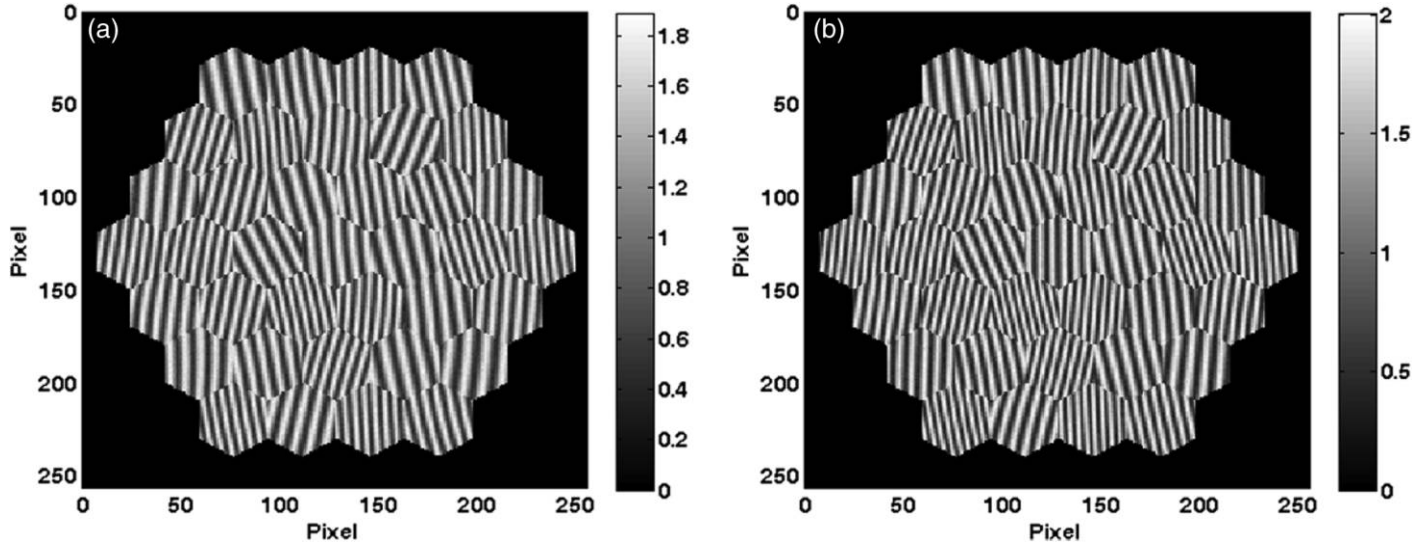

FIG. 8.—Holograms for T2 recorded at the wavelengths of (*a*) 0.632 μm and (*b*) 0.532 μm, with S/N = 20

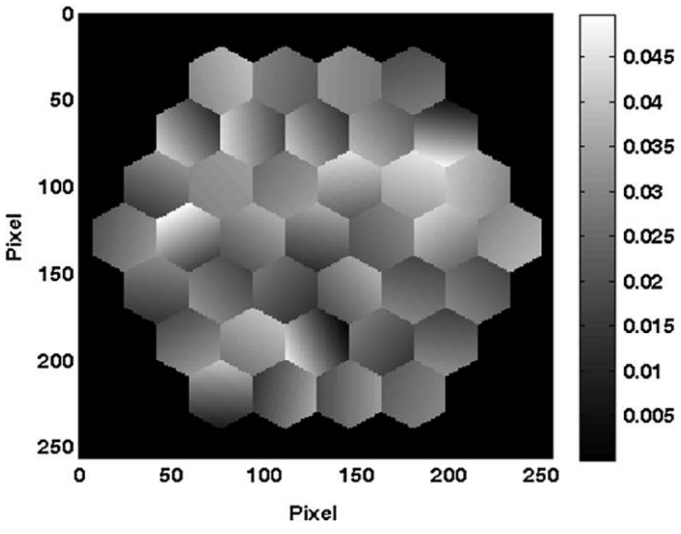

FIG. 10.—Residual height error of T2; the scale is in microns.

0.532 μm in each segment. If the tested wavelength is long enough, for example at the synthetic wavelength, the fringe would disappear, and the phase of T1 can be determined without ambiguity.

According to the procedures of co-phasing segmented telescopes by digital holography described in § 2, the phase of T1 at a longer synthetic wavelength can be obtained using two interferograms, which are recorded at two different wavelengths. Hence, 500 phases, each containing the phase of both T1 and a phase screen, can be gotten at the synthetic wavelength. After averaging the 500 phases, the phase of T1 at the synthetic wavelength is presented in Figure 6. By fitting the plane into the averaged phase of T1 at the synthetic wavelength for each segment using equation (5), the piston and tip/tilt coefficients can be acquired. After repeating this procedure 3 times, co-phasing of T1 in the presence of turbulence and noise can be achieved. Figure 7 shows the residual height error of T1. The PV value of the residual height error of T1 is 0.047 μm, and the rms is 6.83×10^{-3} μm.

4.2. Co-Phasing of T2 by Dual-Wavelength Digital Holography

The procedures of co-phasing of T2 by dual-wavelength digital holography are the same as those for T1. Figure 8 presents two holograms containing the phase information of T2 at the wavelengths of 0.633 and 0.532 μm with $S/N = 20$. As T2 contains not only piston but also tip/tilt errors, the fringe orientations in each segment for T2 change greatly compared with those of *Tip*. The averaged phase of T2 at the synthetic wavelength and the residual height error of T2 are, respectively, shown in Figures 9 and 10. The PV and rms values of the residual height error for T2 are, respectively, 0.050 μm and 6.59×10^{-3} μm.

The simulation results show that the accuracies of co-phasing T1 and T2 by dual-wavelength digital holography are of the same order of magnitude. Hence, this digital holographic approach can remove misalignment errors (including piston and tip/tilt errors) of the segmented telescope with high accuracy.

In practice, the correspondence of segments between the actual telescope and the averaged phase plane can be extracted from the averaged phase of telescope at the synthetic wavelength, as shown in Figures 6 and 9. Once this correspondence is extracted, the coefficients of piston and tip/tilt of each segment can be used for co-phasing the actual telescope.

5. CONCLUSIONS

Online co-phasing of segmented telescopes using dual-wavelength digital holography with the existence of atmospheric turbulence and detection noises has been proposed and numerically tested by two simulated telescopes. By employing the dual-wavelength digital holography technique, the phase of the segmented telescope can be obtained at a longer synthetic wavelength. Fitting the phase plane for each segment of the simulated telescopes, the piston and tip/tilt coefficients of the simulated telescopes can be obtained. The numerical simulations show that the proposed approach for co-phasing of segmented telescopes in the presence of turbulence and noise is very convenient, robust and accurate.

This work is supported by the National Natural Science Foundation of China (Grant Nos. 11203052 and 11373048) and by special funding for the Young Researcher of Nanjing Institute of Astronomical Optics and Technology, CAS. We also wish to thank the anonymous reviewers for their helpful suggestions to improve the paper.

REFERENCES

Angel, J. 1994, Nature, 368, 203
Chanan, G., Ohara, C., & Troy, M. 2000, Appl. Opt., 39, 4706
Chanan, G., Troy, M., Dekens, F., Michaels, S., Nelson, J., Mast, T., & Kirkman, D. 1998, Appl. Opt., 37, 140
Charrière, F., Pavillon, N., Colomb, T., Depeursinge, C., Heger, T. J., Mitchell, E. A. D., Marquet, P., & Rappaz, B. 2006, Opt. Express, 14, 7005
Esposito, S., Pinna, E., Tozzi, A., Stefanini, P., & Devaney, N. 2003, Proc. SPIE, 5169, 72
Gass, J., Dakoff, A., & Kim, M. 2003, Opt. Lett., 28, 1141
Li, C., & Zhang, S. 2012, Proc. SPIE, 8450, 84500B
Mann, C., Bingham, P., Paqit, V., & Tobin, K. 2008, Opt. Express, 16, 9753
Mann, C., Yu, L., Lo, C.-M., & Kim, M. 2005, Opt. Express, 13, 8693

Orlov, V. G., Cuevas, S., Garfias, F., Voitsekhovich, V. V., & Sanchez, L. J. 2000, Proc. SPIE, 4004, 540
Paxman, R., & Fienup, J. 1988, J. Opt. Soc. Am. A, 5, 914
Pizarro, C., Arasa, J., Laguarta, F., Tomàs, N., & Pintó, A. 2002, Appl. Opt., 41, 4562
Roggemann, M. C., Tyler, D. W., & Bilmont, M. F. 1992, Appl. Opt., 31, 7429
Yaitskova, N., Dohlen, K., Dierickx, P., & Montoya, L. 2005, J. Opt. Soc. Am. A, 22, 1093
Yamaguchi, I., Kato, J.-i., Ohta, S., & Mizuno, J. 2001, Appl. Opt., 40, 6177